Calibrated expressions for welding and their application to isotherm width in a thick plate

(Expressões calibradas para soldagem e suas aplicações à largura isotérmica em uma placa plana de largura infinita)

Gentry Wood [1], Shahrukh Al Islam[2], Patricio F. Mendez[3]
[1]Canadian Centre for Welding and Joining, University of Alberta, Edmonton, Alberta, Canada. gentry@ualberta.ca
[2]Canadian Centre for Welding and Joining, University of Alberta Edmonton, Alberta, Canada. saislam1@ualberta.ca
[3]Canadian Centre for Welding and Joining, University of Alberta, Edmonton, Alberta, Canada. pmendez@ualberta.ca

Resumo

O presente artigo apresenta uma solução possível às limitações de soluções modernas de tentativa e erro no desenvolvimento de procedimentos de soldagem. As dificuldades de encontrar soluções generalizadas para a equação de Rosenthal são discutidas e a abordagem de Calibração e Representação Mínima é apresentada como um procedimento promissor para o desenvolvimento destas soluções. Fatores dominantes são identificados, com os efeitos de fenômenos secundários sendo contabilizados por fatores de correção. Os fatores de correção são calibrados e mostrados em uma forma que podem ser facilmente calculados e utilizados pela indústria. A abordagem é, então, demonstrada determinando-se a largura da isoterma através da solução da equação de Rosenthal para uma placa plana. Comparações das equações escalonadas calibradas com a solução exata da equação de Rosenthal mostraram um erro máximo de menos do que 0,8% para qualquer isoterma.

Palavras-chave: *Escalonamento, Equação de Rosenthal, Largura da Isoterma, Soldagem, Desenvolvimento de procedimentos.*

Abstract: *The present paper introduces a possible solution to the limitations of modern trial and error solutions to welding procedure development. The difficulties of finding generalized solutions to Rosenthal's equation are discussed and the Minimal Representation and Calibration approach is introduced as a promising procedure for developing these solutions. Dominant factors are identified, with effects from secondary phenomena being taken into account by correction factors. These correction factors are then calibrated and presented in a form that can be easily computed, and therefore be amendable to industry. The approach is then demonstrated by determining the isotherm width from Rosenthal's thick plate solution. Comparison of the calibrated scaling equations to Rosenthal's exact solution showed a maximum error of less than 0.8% for any isotherm.*

Keywords: *Scaling, Rosenthal Equation, Isotherm Width, Welding, Procedure Development.*

Nomenclature

x:	Position in the x-direction [m]
y:	Position in the y-direction [m]
T:	Temperature [K]
r:	Magnitude of the distance from the origin [m]
w:	Width of the isotherm [m]
Centerline:	Line along the centre of the isotherm (y=0)
η:	Process efficiency
α:	Thermal diffusivity [m^2/s]
Q:	Nominal heat input [W]
k:	Thermal conductivity [W/mK]
T_0:	Preheat [K]

Recebido em 11/08/2014, texto final em 27/08/2014.
DOI: http://dx.doi.org/10.1590/0104-9224/SI1903.03

U:	Travel velocity [m/s]
x^*:	Dimensionless x-coordinate
y^*:	Dimensionless y-coordinate
T^*:	Dimensionless temperature
r^*:	Dimensionless radial distance from the origin
$x_{m_0}{}^*$:	Exact dimensionless x-coordinate of the maximum point of the isotherm
y_m:	y-coordinate of maximum point of the isotherm [m]
$\widehat{y_m}$:	Estimate of the y-coordinate of the isotherm maximum [m]
$\widehat{y_m}^*$:	Estimate of the dimensionless y-coordinate of the isotherm maximum
y_{m_0}:	Exact y-coordinate of the isotherm maximum for (T*≤1) [m]
$\widehat{y_{m_0}}$:	Estimate of the y-coordinate of the isotherm maximum for (T*≤1) [m]
$\widehat{y_{m_0}}^*$:	Estimate of the dimensionless y-coordinate of the isotherm maximum for (T*≤1)
y_{m_∞}:	Exact y-coordinate of the isotherm maximum for (T*>1) [m]
$\widehat{y_{m_\infty}}$:	Estimate of the y-coordinate of the isotherm maximum for (T*>1) [m]
$\widehat{y_{m_\infty}}$:	Estimate of the dimensionless y-coordinate of the isotherm maximum for (T*>1)
$\widehat{y_m}^+$:	Calibrated estimate of the y-coordinate of the isotherm maximum width [m]
$y_{m_0}{}^+$:	Calibrated estimate of the y-coordinate of the isotherm maximum width for (T*≤1) [m]
$\widehat{y_{m_\infty}}^+$:	Calibrated estimate of the y-coordinate of the isotherm maximum width for (T*>1) [m]
$f_{y_{m_e}}(T^*)$:	Correction factor for maximum isotherm width resulting in an exact value
$f_{y_{m_{0,e}}}(T^*)$:	Exact correction factor for (T*≤1)
$f_{y_{m_0}}(T^*)$:	Calibrated correction factor for (T*≤1)
$f_{y_{m_{\infty,e}}}(T^*)$:	Exact correction factor for (T*>1)
$f_{y_{m_\infty}}(T^*)$:	Calibrated correction factor for (T*>1)
C_1, C_2, C_3:	Constants used to calibrate correction factor estimates
$e_{y_{m_0}}$:	Error of the scale isotherm width estimate for (T*≤1)
$e_{y_{m_0}}$:	Error of the scale isotherm width estimate for (T*>1)

1. Introduction

Recent advances in technology have made it possible to consider welding a scientific endeavour rather than an art form [1]. These advancements mean that welders can now make use of plasma arcs, lasers, electron beams, explosives, and mechanical devices to join metals at the atomic level [2]. Despite the enormous progress in the last 30 years, there is a distinct lack of insightful, quantitative, physically relevant guidelines for welding problems [2]. For the most part, an empirical trial and error approach has been used in industry to solve complex welding problems. This approach has only been capable of providing answers in a limited range of real life scenarios, and as a result these answers have not enhanced intuition, creativity, or engineering judgement. At the academic level, numerical simulations have been developed to make meaningful predictions about welding processes. However, due to their complexity and lack of wide scale applicability, they have seen limited acceptance and use by practitioners of industry [3].

The absence of general solutions to welding problems is a result of the complex, multicoupled physics of the process. Typically welding involves many of the issues of thermofluids in addition to electromagnetic body forces, chemical reactions, phase transformations, and complex free surface conditions [3]. The large number of coupled phenomena leads to welding technologies being notoriously difficult to study, be it experimentally of through numerical simulation. This paper presents a promising approach to address the limitations of

empirical experiments and numerical simulations of the past. Complex problems in welding can be tackled using asymptotic expressions and appropriate correction factors. In essence, a complex welding problem can be reduced and solved by inputting parameters into inexpensive and common spreadsheet software. This approach provides an alternative to existing procedure development techniques, which bridges the gap between the complexity of numerical simulations and the exhaustive nature of trial and error qualifications.

The proposed methodology for this asymptotic analysis is a six step procedure called the Minimal Representation and Calibration (MRC) approach. The results of the MRC approach can be calibrated against experiments, numerical models, or exact solutions. In this study, the MRC methodology is introduced and applied to Rosenthal's thick plate equation for isotherm temperature for point heat sources [4]. The relationship between weld parameters and substrate temperature has also been explored by [5-9]. The maximum width of a given temperature isotherm is determined using asymptotic equations (also known as scaling laws), which capture the change in maximum width in a generalized way. Correction factors are then derived to match the exact solution of Rosenthal's equation to the derived expressions. An example has also been included to demonstrate the application of the results of the MRC procedure to a real world welding scenario.

2. Engineering Design Rules: Minimal Representation and Calibration Approach

For a wide range of engineering disciplines, design rules are an essential part of practice. They almost always have the form shown in Equation (1) [3].

$$\textit{(Simple Formula)} \times \textit{(Correction Factor)} \quad (1)$$

The success and generality of Equation (1) can be extended to a variety of engineering problems outside of welding [3]. Examples of such an approach can be found in stress concentration analysis in solid mechanics [10], fluid dynamic drag [11], bearing life calculation [12], and stress in gear teeth [13].

The MRC approach is based on the most idealized conception that is still able to capture the dominant phenomena. Correction factors are the applied to the formula to take into account the most important departures from the ideal case, which can then be calibrated to minimize the deviation between the scaled and exact solutions. Some special features of the MRC approach, which are described in [3], are:

- Predictions made by the MRC approach are made only for characteristic values (such as maximum value of a field), not for whole fields. The dependence that is being studied is not based on the independent variables, but rather on the problem parameters. In a typical welding problem, a characteristic value could be the width of an isotherm, which is demonstrated in subsequent sections, and not the exact magnitude of temperature at any position in space. Characteristic values are studied in further detail in [14].
- Once the correction factors are obtained, they are easy to calculate based on information that is known beforehand. The formula proposed in this paper has the form of a power law, with the correction factors that can be well tabulated. For example, in a welding problem, process efficiency, thermal diffusivity, travel velocity, nominal heat input, thermal conductivity and preheat are known quantities prior to welding. Parameters should not include magnitudes such as molten metal velocity, which can only be determined after simulation or experimentation.
- The correction factors take into account secondary phenomena which are originally discarded during the initial stages of the MRC approach. As such, the correction factors have a physical, real world meaning and applicability.
- The correction factors can be used to determine a limit to the validity of the idealized cases.
- Minimal expressions that are properly calibrated generally reproduce existing experimental data with accuracy comparable to experiments.
- As real world problems approach the idealized case, the correction factors tend to 1 or a constant value of magnitude of 1. Thus the model and reality correspond to a consistent value of the order of 1 to one another in the asymptotic limit.

3. Applying the Minimal Representation and Calibration Approach to a Welding Problem

The MRC approach is able to capture the multicoupled, multiphysics nature of welding. It has the ability to account for a range of phenomena, rather than the case by case experimental expressions often used in industry. This ability ensures generality is achieved. MRC consists of the following steps, which were first proposed in [3]:

1. List all physics considered relevant
2. Identify dominant factors
3. Solve approximate problem considering only dominant factors
4. Check for self-consistency
5. Compare predictions to "reality"
6. Calibrate predictions

To illustrate these steps, the width of an isotherm in a thick substrate using Rosenthal's solution for point heat sources is considered., which is shown in Equations (2) and (3) [4]. Thick plate substrate in this case is defined as a semi-infinite plate where the heat flow is three dimensional.

$$T = T_o + \frac{\eta Q}{2\pi k r} exp\left[-\frac{U}{2\alpha}(r + x)\right] \quad (2)$$

$$r = \sqrt{x^2 + y^2} \quad (3)$$

A graphical representation of this solution is shown in (Figure 1). The x-axis is fixed to the centerline of the moving heat source, and positive x is denoted to be the direction of

motion with the frame of reference attached to the heat source.

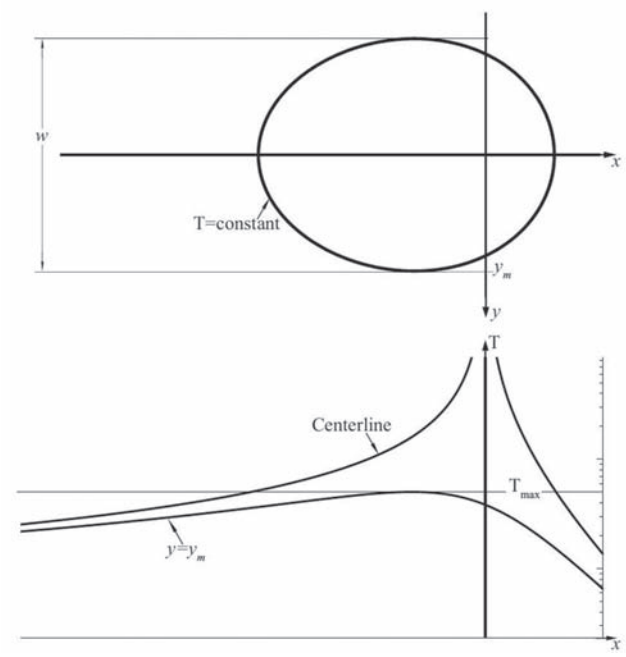

Figure 1. Isotherms and temperature profiles for a point heat source in a thick plate

The independent variables ({X}), dependent variables ({U}), and parameters ({P}) for Rosenthal's thick plate solution are shown in Equations (4)-(6).

$$\{X\}=\{x,y\} \quad (4)$$

$$\{U\}=\{T\} \quad (5)$$

$$\{P\}=\{Q,k,U,\alpha\} \quad (6)$$

Equation (2) can be normalized as follows:

$$T^* = \frac{1}{r^*}\exp(-r^* - x^*) \quad (7)$$

$$r^* = \sqrt{(x^*)^2 + (y^*)^2} \quad (8)$$

Where:

$$x^* = \frac{U}{2\alpha}x \quad (9)$$

$$y^* = \frac{U}{2\alpha}y \quad (10)$$

$$T^* = (T - T_o)\frac{4\pi k\alpha}{\eta QU} \quad (11)$$

The dimensionless groups in Equations (9)-(11) reduce the problem from a total of seven variables down to three variable groups. Note the Equation (8) is not truly independent and is a function of Equations (9) and (10).

The MRC approach is now applied to illustrate how very general power laws can be combined with correction factors to produce the original solution with high accuracy.

3.1 List all physics considered relevant

This list must include dominant phenomena, and may include various secondary phenomena. The following is a list of phenomena that is considered especially relevant in welding problems:

- Conduction: Heat transported by molecular mechanisms in the solid substrate
- Advection: Heat transported due to the relative motion of torch and plate
- Radiation: Heat lost by the hot surface of the substrate
- Convection: Heat transported in the weld pool due to the motion of molten metal
- Phase transformations: Absorption or release of heat due to the transformations from solid to liquid or between different solid-state phases
- Electromagnetic effects: Flow of current in electric welding creates body forces affecting the motion of molten metal

3.2 Identify all dominant factors

The minimal representation of a system is based only on the dominant factors, with the secondary factors being accounted for by the correction factors. Identification of dominant factors is critical and can be formal, intuitive or a combination of both [3].

An inspection of the normalized Rosenthal solution shows that there are two dimensionless independent variables, one dimensionless dependent variable, and no dimensionless parameters. Rosenthal intuitively determined that the following approximations had only secondary effects:

- No fluid flow in the molten pool
- Constant material properties with temperature
- Infinite plate size
- Point heat source
- No convective or radiative heat loss occurs from the surface
- No phase transformations

Rosenthal analysis considers only two mechanisms of heat transfer, i.e. conduction and advection, establishing two asymptotic regimes depending on which mechanism dominates. These two regimes are consistent with the solution of Equation (7), where, for a characteristic value such as isotherm width, there is a relationship between two dimensionless groups only. The two regimes in Rosenthal's solution can be captured by the value of T*. For high values of T* (T* >> 1) conduction is dominant, while for low values of T* (T* << 1) advection is dominant. These two regimes also correspond to what are often called "slow" and "fast" moving heat sources respectively.

3.3 Solve approximate problems using dominant factors

The problem is simplified when only dominant factors are considered, and the solutions can be numerical, exact, or approximate. For the example considered here, there are two regimes each characterized by a different dominant phenomena. At T* >> 1 conduction governs isotherm size, while at T* << 1 advection is dominant. A good estimate for the maximum isotherm width has the following general form applicable to both regimes:

$$y_m = \widehat{y_m} f_{y_{m_e}}(T^*) \tag{12}$$

where $\widehat{y_m}$: is an asymptotic solution to the problem, and $f_{y_{m_e}}$ is a correction factor that would result in the exact value.

The estimate $\widehat{y_m}$: is derived separately for the low and high *T** regimes. The key difference for the estimates is the characteristic shape of the isotherm in the asymptotes of the *T** domain. For low *T** values the isotherms become increasingly elongated due to the dominant effect of advection, and at high *T** values the isotherms become circular as conduction dominates and the heat is dissipated equally in the *(xy)** plane.

Low *T Regime**

Equation (12) can be rewritten using the following notation for low *T** values:

$$y_m = \widehat{y_{m_o}} f_{y_{m_{0,e}}}(T^*) \tag{13}$$

where $\widehat{y_{m_o}}$ is the estimate for the asymptotic regime when *T** approaches 0 (advection dominant) and $f_{y_{m_{0,e}}}$ is the correction factor that results in an exact solution for $T^* \leq 1$.

For the fast moving heat source, the elongated isotherms have a much larger length to width ratio and satisfy the condition $y^*/x^* << 1$. Equation (3) can be rearranged in terms of y^*/x^* by factoring $(x^*)^2$ from underneath the square root. Only the negative solution of $|x^*|$ is considered for this analysis because the maximum width will always occur at a negative *x** position. For $x^* < 0$ Equation (3) becomes:

$$r^* = -x^* \sqrt{1 + \left(\frac{y^*}{x^*}\right)^2} \tag{14}$$

Using the first two terms of an expansion of the square root around1, Equation (14) can be transformed to the following form:

$$r^* \approx -x^* \left[1 + \frac{1}{2}\left(\frac{y^*}{x^*}\right)^2\right] \tag{15}$$

By multiplying the equation by -1 and subtracting *x** from both sides, the left side of the equation represents the argument of the exponential of Equation (7).

$$-r^* - x^* \approx x^* \left[1 + \frac{1}{2}\left(\frac{y^*}{x^*}\right)^2\right] - x^* \tag{16}$$

Multiplying the *x** term through and simplifying the results, we arrive at the following form of the approximation:

$$-r^* - x^* \approx -\frac{1}{2}\frac{(y^*)^2}{x^*} \tag{17}$$

Substituting Equation (17) into Equation (7) yields an expression for low *T** values in terms of both *x** and *y**:

$$T^* \approx \frac{1}{x^*} exp\left[-\frac{1}{2}\frac{(y^*)^2}{x^*}\right] \tag{18}$$

Differentiation of Equation (18) with respect to *x**, leads to the resulting expression:

$$\frac{\partial T^*}{\partial x^*} = \frac{\exp\left[\frac{(y^*)^2}{x^*}\right][2x^* - (y^*)^2]}{2(x^*)^3} \tag{19}$$

By setting $\partial T^*/\partial x^* = 0$, the location of the dimensionless estimate of maximum *y** at low *T** values, denoted as $\widehat{y_{m_0}}^*$, can be determined, which after simplification leads to a direct relationship between $\widehat{y_{m_0}}^*$ in terms of the dimensionless x coordinate at the maximum $x_{m_0}{}^*$.

$$x_{m_0}{}^* = \frac{\left(\widehat{y_{m_0}}^*\right)^2}{2} \tag{20}$$

By substituting Equation (20) into Equation (18), a relationship of $\widehat{y_{m_0}}^*$ as a function of only *T** can be established. The significance of this relationship is that isotherm width can now be expressed exclusively by a single dimensionless parameter.

$$\widehat{y_{m_0}}^* = \sqrt{\frac{2}{eT^*}} \tag{21}$$

By inputting the parameters of *T** from Equation (11) into Equation (21), the following expression is obtained, which equates the estimate of dimensionless isotherm width exclusively in terms of welding parameters.

$$\widehat{y_{m_0}}^* = \sqrt{\frac{e^{-1}\eta QU}{2\pi k\alpha(T - T_0)}} \tag{22}$$

By substituting Equation (10) into Equation (22), we can develop an expression for the dimensional estimate $\widehat{y_{m_0}}$ for low *T** values.

$$\widehat{y_{m_0}} = \sqrt{\frac{2e^{-1}\alpha\eta Q}{\pi kU(T - T_0)}} \tag{23}$$

Inserting the above result into Equation (13) gives us an expression for the exact solution $\widehat{y_{m_0}}$ in terms of the derived approximation multiplied by a correction factor for low *T** values.

$$y_{m_0} = \sqrt{\frac{2e^{-1}\alpha\eta Q}{\pi kU(T - T_0)}} f_{y_{m_{0,e}}} \tag{24}$$

High *T Regime**

Similar to low *T**, the general formula for can be expressed using notation for high *T** values:

$$y_m = \widehat{y_{m_\infty}} f_{y_{m_{\infty,e}}}(T^*) \quad (25)$$

where $\widehat{f_{y_{m_\infty}}}$ is the estimate for the asymptotic regime when T^* approaches infinity (conduction dominant) $f_{y_{m_{\infty,e}}}$ and is the correction factor that result in an exact solution for $T^* > 1$.

At high T^* values, Rosenthal's solution predicts that the isotherm takes the shape of a circle centred at the heat source. Equation (7) therefore reduces to the approximate form below:

$$T^* \approx \frac{1}{r^*} \quad (26)$$

At the maximum point of the isotherm for high T^* values, $x^* = y_{m_\infty}{}^* = 0$, leaving only the y^* component of r^*, which is denoted . This leads to the following expression for $\widehat{y_{m_\infty}}^*$ in terms of only T^*.

$$\widehat{y_{m_\infty}}^* = \frac{1}{T^*} \quad (27)$$

Substituting the values from Equation (11) into Equation (27), an expression for $\widehat{y_{m_\infty}}^*$ is obtained in terms of welding process variables for a given temperature.

$$\widehat{y_{m_\infty}}^* = \frac{\eta Q U}{4\pi k \alpha (T - T_0)} \quad (28)$$

The above equation can be rearranged to dimensional form by substituting Equation (10) as follows:

$$\widehat{y_{m_\infty}} = \frac{\eta Q}{2\pi k (T - T_0)} \quad (29)$$

Inserting the results of Equation (29) into the general expression for y_m for high T^* values, we obtain an expression for the exact solution of y_{m_∞} as a function of the derived estimate multiplied by the correction factor for high T^* values.

$$y_{m_\infty} = \frac{\eta Q}{2\pi k (T - T_0)} f_{y_{m_{\infty,e}}} \quad (30)$$

3.4 Check for self consistency

In this simple uncoupled example, self-consistency is not a problem. The consideration of only two relevant phenomena guarantees that when one phenomenon is neglected the other will govern system behaviour. For more complex scenarios involving three of more coupled phenomena, it is necessary to confirm that the secondary factors are of secondary importance and magnitude. By computing the value of terms in the governing equation using the estimate of the characteristic value, the significance of neglected phenomena can be evaluated. The simple case applies to maximum isotherm width using Rosenthal's equation, where advection and conduction are the only two relevant phenomena under consideration.

3.5 Compare predictions to reality

It is important that scaling laws are validated through comparison with reality. Reality for this example is considered to be Rosenthal's exact solution. The exact correction factors for high and low T^* regimes can be derived from the ratio of the exact to estimate solutions for maximum isotherm width, which is described in detail in this section.

Low T^* Regime

The exact correction factor for $T^* < 1$, $f_{y_{m_{0,e}}}$, can be mathematically described by the ratio of the exact solution to the estimate solution. Taking advantage of this definition, the exact correction factor can also be represented by the ratio of the dimensionless exact solution and dimensionless estimate as both multiplied by the same normalizing factor.

$$f_{y_{m_{0,e}}}(T^*) = \frac{y_{m_0}{}^*}{\widehat{y_{m_0}}^*} \quad (31)$$

Substituting the relationship established in Equation (21) into Equation (31), we arrive at the following expression for $f_{y_{m_{0,e}}}$, which depends only on T^*:

$$f_{y_{m_{0,e}}}(T^*) = \sqrt{\frac{e}{2}} y_{m_0}{}^* \sqrt{T^*} \quad (32)$$

High T^* Regime

Similar to the low T^* regime, the exact correction factor for high T^* values, $f_{y_{m_{\infty,e}}}$ is defined as the following ratio of the dimensionless exact solution to dimensionless estimate:

$$f_{y_{m_{\infty,e}}}(T^*) = \frac{y_{m_\infty}{}^*}{\widehat{y_{m_\infty}}^*} \quad (33)$$

Inserting the relationship from Equation (27) into Equation (33), the following expression for $f_{y_{m_{\infty,e}}}$ as a function of only T^* is established:

$$f_{y_{m_{\infty,e}}}(T^*) = y_{m_\infty}{}^* T^* \quad (34)$$

As $f_{y_{m_{0,e}}}$ approaches $T^* << 1$ and $f_{y_{m_{\infty,e}}}$ approaches $T^* >> 1$, the exact correction factors tend to 1, which indicates the estimates are good in the asymptotes of each regime. This behaviour is shown in (Figure 2).

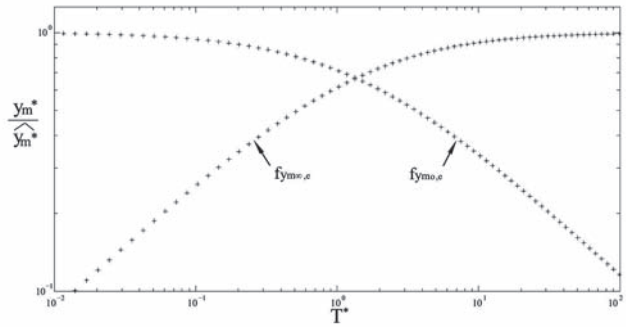

Figure 2. Exact correction factors for y_m as a function of T^*. $f_{y_{m_{0,e}}}$ is the correction factor for the low T^* regime and $f_{y_{m_{\infty,e}}}$ is for the high T^* regime

3.6 Calibrate predictions

The exact correction factors can be approximated with an appropriate function resulting in a high quality estimate based only on parameters known beforehand, which has the following general form:

$$\widehat{y_m}^+ = \widehat{y_m} f_{y_m} \tag{35}$$

where f_{y_m} is the approximate correction factor, and $\widehat{y_m}^+$ is the corrected asymptotic estimate.

The exact correction factors, $f_{y_{m_{0,e}}}$ and $f_{y_{m_{\infty,e}}}$, both depend only on T^* and can be approximated using the expression shown in Equations (36) and (37) respectively. This approach has also been used by Churchill et al. for developing general asymptotic solutions for phenomena that vary between limiting cases [15].

$$f_{y_{m_0}}(T^*) = [1 + (C_1 T^*)^{C_3}]^{\frac{C_2}{C_3}} \tag{36}$$

$$f_{y_{m_\infty}}(T^*) = \left[1 + \left(\frac{C_1}{T^*}\right)^{C_3}\right]^{\frac{C_2}{C_3}} \tag{37}$$

The calibrated form of the isotherm width equation can be expressed for $\widehat{y_{m_0}}^+$ $\widehat{y_{m_\infty}}^+$ as follows:

$$\widehat{y_{m_0}}^+ = \widehat{y_{m_0}} f_{y_{m_0}} \tag{38}$$

$$\widehat{y_{m_\infty}}^+ = \widehat{y_{m_\infty}} f_{y_{m_\infty}} \tag{39}$$

The graphical solution of the calibrated correction factors compared to the exact correction factors is shown in (Figure 3). Both calibrated factors who excellent agreement for all T^* values, which extends beyond their region of intended use.

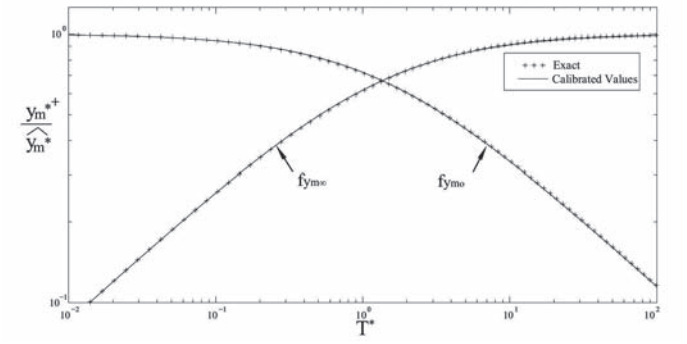

Figure 3. Comparison of the exact correction factors to the calibrated correction factors. The maximum error is below 0.8%

The form of the calibrated correction factors is such that it matches the behaviour of the exact correction factors in the asymptotes with only slight deviations in the intermediate region around $T^* = 1$. The calibrated correction factor $f_{y_{m_0}}$ tends to 1 at low T^* values $T^* << 1$ where the T^* term is negligible and approaches $(C_1 T^*)^{C_2}$ at high T^* values where the T^* term dominates. For $f_{y_{m_\infty}}$ the calibrated approximation tends to 1 as T^* becomes large and approaches $\left(\frac{C_1}{T^*}\right)^{C_2}$ at low T^* values.

The calibrated correction factors include three constants to match the behaviour of the exact correction factors. The values of C_1 and C_2 come directly from the derivation shown in step 5, but the constant C_3 has been included to provide an additional degree of manipulation in the intermediate region near $T^* = 1$. This manipulation has been accomplished while preserving the behaviour of the correction factors in the asymptotes of both regimes for both correction factors.

The error between the exact and calibrated factors has been calculated using a ratio of logs to better represent the difference across large orders of magnitude. The formula for error for $f_{y_{m_0}}$ and $f_{y_{m_\infty}}$ are shown in Equations (40) and (41).

$$e_{y_{m_0}} = \ln \frac{f_{y_{m_{0,e}}}(T^*)}{f_{y_{m_0}}(T^*)} \tag{40}$$

$$e_{y_{m_\infty}} = \ln \frac{f_{y_{m_{\infty,e}}}(T^*)}{f_{y_{m_\infty}}(T^*)} \tag{41}$$

Using the definition of Equations (40) and (41), plots such as the one in (Figure 4) can be generated for a wide range of C_3 values. It is noted that the maximum and minimum observed in (Figure 4) are symmetric about the T^* axis.

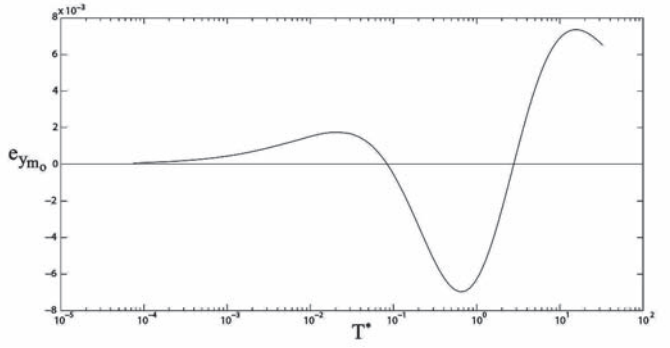

Figure 4. Error as a function of T^* for $f_{y_{m_0}}$ and $C_3 = 0.865$

The absolute maximum error for a large range of C_3 values was then plotted to determine a C_3 that minimizes the maximum error. A minimum was identified at $C_3 = 0.865$ correct to three significant digits for $f_{y_{m_0}}$ and $f_{y_{m_\infty}}$. The graph for error minimization of $f_{y_{m_0}}$ is shown in (Figure 5).

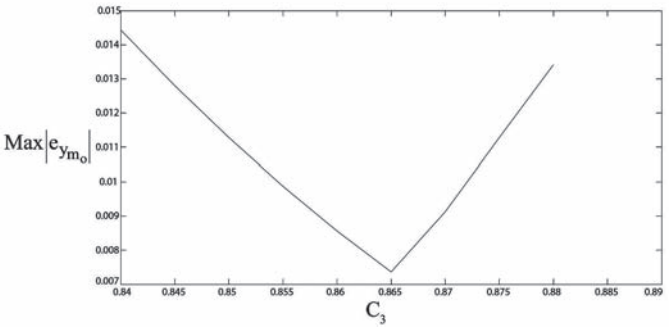

Figure 5. Identification of C_3 to minimize the absolute error of $f_{y_{m_0}}$

This approach to calibrating the correction factors has been highly successful, as shown by the excellent fit of the exact and calibrated values in (Figure 3). The maximum absolute error for both correction curves is less than 0.8% corresponding to an accuracy of at least 99.2% for any isotherm. Table 1 summarizes the values of C_1, C_2 and optimized C_3 for both correction factors.

Table 1. Values of optimized calibration constants for $f_{y_{m_0}}$ and $f_{y_{m\infty}}$

	Equation Number	C_1	C_2	C_3
$f_{y_{m_0}}$	(36)	$\frac{2}{e}$	-0.5	0.865
$f_{y_{m\infty}}$	(37)	$\frac{e}{2}$	-0.5	0.865

4. Sample Calculation

To demonstrate the procedure for applying correction factors, a sample welding scenario is presented to calculate the width of the 800°C isotherm during welding of AISI 1010 carbon steel with no preheat. Recommended welding parameters for GMAW of carbon and low alloy steels using 100% CO_2 shielding gas from the Lincoln GMAW welding catalogue have been selected for this example [16]. Parameters for 3 mm plate and 0.9 mm diameter electrode are: 21 V DC+, 0.5 m/min travel speed, and approximately 160 A. The arc efficiency for this process has been cited as 85% [17]. Relevant material data for AISI 1010 at 300 K include a = 18.8∗10^{-6} m^2/s and k = 63.9 W/mK [18].

The first step using this approach is to determine the value for the particular problem, which is done using Equation (11). The value of was calculated to be 0.492.

$$T^* = (T - T_o)\frac{4\pi k\alpha}{\eta QU} \tag{11}$$

$$T^* = (1073\,K - 298\,K)\frac{4\pi(63.9\,W/mK)(18.8 * 10^{-6}\ m^2/s)}{(0.85)[(21\,V)(160\,A)](0.00833\ m/s)}$$

$$T^* = 0.492$$

Since this value is lower than one, advection is the dominating phenomenon. Equation (23) is used to calculate the estimate of isotherm width $\widehat{y_{m_0}}$, which is 5.520 mm for this example.

$$\widehat{y_{m_0}} = \sqrt{\frac{2e^{-1}\alpha\eta Q}{\pi kU(T - T_0)}} \tag{23}$$

$$\widehat{y_{m_0}} = \sqrt{\frac{2e^{-1}(18.8 * 10^{-6}\ m^2/s)\,(0.85)[(21\,V)(160\,A)]}{\pi(63.9\,W/mK)(0.00833\ m/s)(1073\,K - 298\,K)}}$$

$$\widehat{y_{m_0}} = 5.520\,mm$$

The correction factor for low T^* values, $f_{y_{m_0}}(T^*)$, is found using Equation (36) and the calibrated constants in Table (1). $f_{y_{m_0}}(T^*)$ is shown to be 0.818 for a T^* value of 0.492.

$$f_{y_{m_0}}(T^*) = [1 + (C_1T^*)^{C_3}]^{\frac{C_2}{C_3}} \tag{36}$$

$$f_{y_{m_0}}(0.492) = \left[1 + \frac{2}{e}(0.492)^{0.865}\right]^{\frac{-0.5}{0.865}}$$

$$f_{y_{m_0}}(0.492) = 0.818$$

Combining the estimate $\widehat{y_{m_0}}$ and the correction factor $f_{y_{m_0}}(T^*)$ using Equation (38), we find that the calibrated estimate for maximum width of the 800°C isotherm from the origin is 4.517 mm.

$$\widehat{y_{m_0}}^{+} = \widehat{y_{m_0}} f_{y_{m_0}} \tag{38}$$

$$\widehat{y_{m_0}}^{+} = (5.520\,mm)(0.818)$$

$$\widehat{y_{m_0}}^{+} = 4.517\,mm$$

The application of the MRC approach to isotherm width has been demonstrated using the series of equations shown in this sample calculation and information that is known prior to welding. The general nature of the developed expressions allows this approach to be extended to any number of welding processes, materials, and parameter combinations as an excellent starting point approximation of isotherm width prior to experimental trials.

5. Discussion

The MRC approach provides for the first time a framework for systematically determining reliable estimates for characteristic values of welding systems that match the exact solution. The rigorous systematic aspect of this work relies on representing system behaviour in the asymptotic cases using scaling estimates, and applying correction factors to account for deviations from the asymptotic limit.

Based on the analysis of maximum isotherm width presented here, there is error associated with neglecting the secondary terms in the scaling expressions. For this simple uncoupled example, the exclusion of either advection or conduction was shown to have a negligible impact in the asymptotic cases where the scaling estimates match the exact solution. The implementation of calibrated correction factors compensated for the intermediate regime where advection and conduction are of comparable magnitude and resulted in a maximum error of 0.8% between the estimate and exact solution for any isotherm. Unexpectedly, the correction factors $f_{y_{m_0}}$ and $f_{y_{m\infty}}$ had excellent agreement across all T^* values, which implies they could be successfully used outside of their intended dominant regime.

6. Conclusions

A 6 step Minimal Representation and Calibration approach was presented as a promising alternative to current welding procedure development techniques. The six steps are:

1. List all physics considered relevant
2. Identify dominant factors

3. Solve approximate problem considering only dominant factors
4. Check for self-consistency
5. Compare predictions to "reality"
6. Calibrate predictions

The MRC approach was applied to determine the maximum isotherm width from Rosenthal's thick plate solution for a point heat source (Equation (2)). Through a series of non –dimensional transformations, a set of two independent dimensionless groups were identified that completely characterized the maximum width of any isotherm (x^*, y^*). Two regimes for the dimensionless dependent group T^* were present based on the dominant physics governing system behaviour in the regime. At low values of T^* ($T^* << 1$), advection was dominant, and at high T^* ($T^* >> 1$) conduction controlled maximum isotherm width. Considering the isotherm shape difference in the respective T^* regimes, two scaling laws, one for each regime, were derived, which captured the exact isotherm width as a function of T^*. The results of these derivations are shown in Equations (24) and (30) for low and high T^* respectively. The developed asymptotic expressions were based only on process variables that are typically known prior to welding allowing them to be used for predictive purposes prior to experimental trials.

As part of the MRC methodology, correction factors were derived to ensure an exact match of the asymptotic expressions to the exact solution for isotherm width for both regimes. The derived factors were also estimated as power laws, which depended only on and 3 scaling constants. The values of the constants were chosen to minimize the maximum error between the exact and estimate solutions for isotherm width. Theses calibrated correction factors yielded a maximum error of less than 0.8% demonstrating an excellent agreement between the asymptotic expressions and actual solution for any isotherm. An example problem using tabulated welding parameters for a GMAW bead on plate weld was performed to demonstrate the straight forward application of the developed expressions to a real world welding problem.

Overall, the isotherm width problem shows that the MRC approach can be used to tackle complex welding problems in a formal way. It is reasonable to believe that this methodology can be successfully applied to more complex, multicoupled, multiphysics systems.

7. Acknowledgements

This work was partially supported by the Natural Sciences and Engineering Research Council of Canada (NSERC). Valuable discussions and feedback from N. Barnes are gratefully acknowledged. Special thanks to Márcio Corrêa de Carvalho for his help with translation of parts of this work into Portuguese.

8. References

[1] EAGER, T.W. Welding and joining: Moving from art to science. Welding Journal, p.49-55, 1995.
[2] MENDEZ, P.F. Synthesis and generalization of welding fundamentals to design new welding technologies: status, challenges and a promising new approach. Science and Technology of Welding and Joining, v.16, 348 p., 2011.
[3] MENDEZ, P.F.; TELLO, K.E.; GAJAPATHI, S.S. Generalized and communication of welding simulations and experiments using scaling analysis. In: TRENDS IN WELDING RESEARCH, 2012, Chicago. Proceedings of the 9th International Conference, 2012. 249 p.
[4] ROSENTHAL, D. The theory of moving sources and its application to metal treatments. Transactions of A.S.M.E., v.68, p.849-866, 1946.
[5] BROWN, P.E.; ADAMS, C.M. Mathematical theory of heat distribution during welding and cutting. Weld. J., v.20, p.210-215, 1941.
[6] UYEHARA, O.A.; MYERS, P.S.; BORMAN, G.L. The theory of moving sources and its application to metal treatments. Weld. Res. Bull., p.123,1-46 1967.
[7] ASHBY, M.F.; EASTERLING, K.E. The transformation hardening of steel surface by laser beams. Acta Metall., v.32, p.1935-1948, 1984.
[8] GRONG, O.; CHRISTENSEN, N. Effects of weaving on temperature distribution in fusion welding. Mater. Sci. Tech., v.2, p.967-973, 1986.
[9] MYHER, O.; GRONG, O. Dimensionless maps for heat flow analyses in fusion welding. Acta Metall. Mater., v.38, p.449-460, 1990.
[10] PETERSON, R.E.; PILKEY W.D.; PILKEY D.F. Peterson's stress concentration factors. Hoboken: John Wiley, 2008.
[11] HOERNER, S.F. Fluid-dynamic drag; practical information on aerodynamic drag and hydrodynamic resistance. In: Hoerner Fluid Dynamics. Midland Park, N.J., 1965.
[12] Quality Bearing Components, Catalog B620, 2012.
[13] Stock drive products/sterling instrument. Handbook of METRIC Drive Components D805, 2010.
[14] MENDEZ, P.F. Characteristic values in the scaling of differential equation in engineering, Journal of Applied Mechanics, v.77, p.6-17, 2010.
[15] CHURCHILL, S.W.; USAGI, R. A general expression for the correlation of rates of transfer and other phenomena. AIChE, v.18, n. 3, p.1121-1127, 1972.
[16] KOTECKI, D. et al., D. Gas Metal Arc Welding Guidelines. Lincoln Electric.
[17] DUPONT, J.N.; MARDER, A.R. Thermal efficiency of arc welding processes. Welding Journal, v.74, n. 12, p.406-s-416-s, 1995.
[18] BERGMAN, T.L. et al., Fundamentals of Heat and Mass Transfer. 6.ed. John Wiley and Sons, 2007.